The Dynamic Stress Intensity Factor Due to Arbitrary Screw Dislocation Motion

L. M. Brock
Department of Engineering Mechanics,
University of Kentucky,
Lexington, Ky. 40506
Mem. ASME

The dynamic stress intensity factor for a stationary semi-infinite crack due to the motion of a screw dislocation is obtained analytically. The dislocation position, orientation, and speed are largely arbitrary. However, a dislocation traveling toward the crack surface is assumed to arrest upon arrival. It is found that discontinuities in speed and a nonsmooth path may cause discontinuities in the intensity factor and that dislocation arrest at any point causes the intensity factor to instantaneously assume a static value. Morever, explicit dependence on speed and orientation vanish when the dislocation moves directly toward or away from the crack edge. The results are applied to antiplane shear wave diffraction at the crack edge. For an incident step-stress plane wave, a stationary dislocation near the crack tip can either accelerate or delay attainment of a critical level of stress intensity, depending on the relative orientation of the crack, the dislocation, and the plane wave. However, if the incident wave also triggers dislocation motion, then the delaying effect is diminished and the acceleration is accentuated.

Introduction

Bilby and Eshelby [1] have noted the possible role of dislocations in fracture. Simlarly, Rice and Thomson [2], Tirosh and McClintock [3], Burns and Majumdar [4], and Thomson and Sinclair [5] have related fracture initiation to dislocation nucleation and assembly near an existing crack.

In elasticity theory, the stress intensity factor is a key parameter in characterizing fracture initiation. Moreover, if the fracture process is dynamic, the motion of the dislocations should be considered in applying mechanisms such as those in [2–5]. This paper, therefore, attempts to gain insight into the role of dislocations in dynamic fracture by (1) studying the effects of a moving screw dislocation on the dynamic stress intensity factor generated for a stationary crack and (2) applying the information gained to the problem of stress wave diffraction at the crack edge.

Because engineering and geological materials are often assemblies of crystalline grains that may contain local distortions, dislocation paths in a small region such as around a crack edge may not be rectilinear. Therefore, the study considers a screw dislocation that moves from equilibrium along a continuous, piecewise-smooth path. Its speed is subsonic and nonuniform, although the Johnston-Gilman [6] observations that inpath acceleration effects may be negligible should be noted. The dislocation is of unit strength, the crack is semi-infinite, and, as a first step, the cracked material is isotropic, homogeneous, linearly elastic, and unbounded. The dislocation is allowed to travel to the crack surface, but is assumed to arrest upon arrival. The dynamic stress intensity factor is derived and examined for dependence on dislocation position, orientation, and speed.

The study results are then applied to the problem of a screw dislocation near a crack edge at which antiplane shear wave diffraction occurs. The diffraction-dislocation interaction in the crack edge stress field is examined for its fracture initiation implications. Both the stationary dislocation and a dislocation which, triggered by the wave pattern, moves to the crack edge are considered.

The basic problem is analyzed beginning in the next section. The dislocation is represented by an equivalent body force distribution, following [7]. The existence of a characteristic length implies a Wiener-Hopf problem of a nonstandard type. It is advantageous, therefore, to obtain the exact solution by means of the superposition scheme outlined in the following section. This scheme was also used in [8] for the calculation of the dislocation motion-induced portion of the intensity factor when the path is strictly rectilinear.

Basic Problem Formulation

Consider the unbounded elastic plane containing the crack and screw dislocation shown in Fig. 1(*a*). In terms of the Cartesian coordinates (x,y) the crack surface is defined by $y=0$, $x<0$. It is convenient to define the dislocation as the cut

Contributed by the Applied Mechanics Division for presentation at the 1983 ASME Applied Mechanics, Bioengineering, and Fluids Engineering Conference, Houston, Texas, June 20–22, 1983 of THE AMERICAN SOCIETY OF MECHANICAL ENGINEERS.

Discussion on this paper should be addressed to the Editorial Department, ASME, United Engineering Center, 345 East 47th Street, New York, N.Y. 10017, and will be accepted until two months after final publication of the paper itself in the JOURNAL OF APPLIED MECHANICS. Manuscript received by ASME Applied Mechanics Division, April, 1982; final revision, October, 1982. Paper No. 83-APM-21.

Copies will be available until February, 1984.

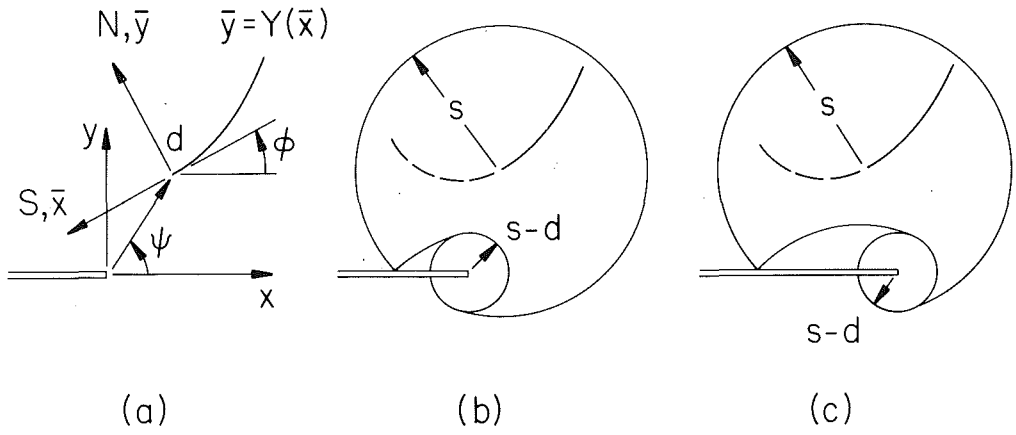

Fig. 1 *(a)* **Initial crack-screw dislocation configuration; *(b)* wave pattern for $|\psi|<\pi/2$; and (c) wave pattern for $|\psi|>\pi/2$**

$N=0$, $S<0$ where (S, N) are tangential and normal coordinates along the dislocation path $\bar{y}=Y(\bar{x})$. As seen in Fig. 1(*a*), the Cartesian coordinates $(\bar{x},\bar{y})$ are centered at the dislocation edge so that the $(\bar{x},S)$ and $(\bar{y},N)$-directions, respectively, coincide there. If ϕ is the path slope at the dislocation edge w.r.t. the crack plane and (d,ψ) are the plane polar coordinates of the dislocation edge w.r.t. the crack edge then

$$\bar{x}=d\cos\Omega-x\cos\phi-y\sin\phi, \quad \bar{y}=d\sin\Omega-x\sin\phi+y\cos\phi,$$
$$\Omega=\phi-\psi \tag{1}$$

We first examine continuous, piecewise-smooth, single-valued path functions Y. Therefore, $|Y'|$ is finite, where $(\,)'$ denotes argument differentiation, while the path-length

$$S=\int_0^{\bar{x}}\sqrt{[1+(Y')^2]}du \tag{2}$$

has a single-valued inverse $\bar{x}=X(S)$. The single-valuedness restriction will eventually be relaxed. For $s<0$, where $s=c\bar{x}$(time) and c is the shear wave speed, the dislocation and crack are in equilibrium. For $s>0$ the dislocation moves along the path $\bar{y}=Y(\bar{x})$ and is located at $N=0$, $S=D(s)$. Here $D(s)$ is continuous, where $D(0)=0$, $0\le\dot{D}<1$, $\dot{(\,)}\equiv\partial(\,)/\partial s$, and the last inequality assures a subsonic speed. If the dislocation reaches the crack surface at some $s=t_0>0$, we require that $\dot{D}(s)=0$, $D(s)=D(t_0)$ for all $s>t_0$. This motion generates a cylindrical shear wave. As seen in Fig. 1(*b*), if $|\psi|<\pi/2$ this wave will first reach the crack edge and there generate a diffracted shear wave. As seen in Fig. 1(*c*), if $|\psi|>\pi/2$ the wave is first reflected by the crack surface itself.

The equations governing the motion are

$$\nabla^2 w+\frac{b}{\mu}=\ddot{w}, \quad \tau_y=0 \quad (y=0, \quad x<0), \quad w\equiv w_0\,(s\le 0) \tag{3}$$

$$\tau_y=w_{,y}, \quad b=\mu H[D(s)-S]\delta'(N) \tag{4}$$

where $w(x,y,s)$ is the antiplane displacement, w_0 is its equilibrium value, μ is the shear modulus, ∇^2 is the Laplacian operator, and $(\,)_{,u}\equiv\partial(\,)/\partial u$. The quantity b is the body force equivalent of the screw dislocation of unit strength while H and δ are the Heaviside and Dirac functions. It is convenient to introduce the superposition

$$w=w_b+w_c+w_0 \tag{5}$$

$$\nabla^2 w_b+\frac{1}{\mu}(b-b_0)=\ddot{w}_b, \quad b_0=\mu H(-S)\delta'(N),$$
$$w_b\equiv 0\,(s\le 0) \tag{6}$$

where b_0 is the initial dislocation equivalent. In view of (3)–(6), then, w_c must satisfy the equations

$$\nabla^2 w_c=\ddot{w}_c, \quad \tau_{yc}=-\tau_{yb}\,(y=0,x<0), \quad w_c\equiv 0 \quad (s\le 0) \tag{7}$$

Equations (6) are the relations governing the displacement w_b due to a body force $b-b_0$ applied in an unbounded, uncracked elastic plane while (7) are those for a displacement w_c generated by the sudden imposition of tractions $-\tau_{yb}$ along a crack $y=0$, $x<0$. This latter field will contain the information about the dynamic stress intensity factor. The general solution for w_b is given in the next section.

General Solution for Dislocation

In view of the dependence of $b-b_0$ and the invariance of ∇^2, it is convenient to seek the function $w_b(\bar{x},\bar{y},s)$. The Laplace transform over s, the Fourier transform over $\bar{x}$ and its inverse are given by, see Sneddon [9]

$$g_L=\int_0^\infty g(s)e^{-ps}ds; \quad g_B=\int_{-\infty}^{\infty} g(\bar{x})e^{-ipq\bar{x}}d\bar{x},$$
$$g(\bar{x})=\frac{p}{2\pi}\int_\Gamma g_B e^{ipq\bar{x}}dq \tag{8a-c}$$

respectively, where p is real, positive, and large enough to insure convergence of (8*a*), q is, in general, complex, and Γ is the inversion integral path. Application of (8*a*,*b*) to (6) in view of appropriate radiation conditions yields

$$\hat{w}_{b,\bar{y}\bar{y}}-p^2a^2\hat{w}_b=\frac{1}{\mu}(\hat{b}_0-\hat{b}), \quad a=\sqrt{(1+q^2)} \tag{9}$$

where $\hat{(\,)}\equiv(\,)_{BL}$ and a is defined in the q-plane cut along $Re(q)=0$, $|Im(q)|>1$, such that $Re(a)\ge 0$. It can be shown that the solution to (9) which is bounded for $|\bar{y}|\to\infty$ is, in view of (4) and (6),

$$2p\hat{w}_b=-\int_0^\infty \dot{D}\frac{dX}{dS}[\mathrm{sgn}(Y-\bar{y})-i\frac{q}{a}Y']$$
$$\cdot e^{-p(t+iqX+a|Y-\bar{y}|)}dt, \quad \frac{dX}{dS}=\frac{1}{\sqrt{[1+(Y')^2]}} \tag{10a,b}$$

where it is understood that $Y=Y(X)$, $X=X(D)$, and $D=D(t)$. Substitution of (10) in (8*c*) gives

$$4\pi w_{bL}=-\int_0^\infty \dot{D}\frac{dX}{dS}e^{-pt}\int_\Gamma[\mathrm{sgn}(Y-\bar{y})-i\frac{q}{a}Y']$$
$$e^{p[iq(\bar{x}-X)-a|Y-\bar{y}|]}dqdt \tag{11}$$

where Γ can be taken along the $Re(q)$-axis. By following the work of deHoop [10], the Cauchy theorem is used to alter the integration path to the q-plane contour along which the

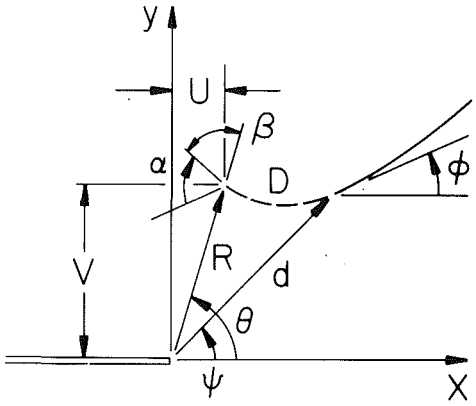

Fig. 2 Instantaneous crack-screw dislocation configuration

imaginary part of the p-factor vanishes while the real part is negative. Then, it is readily shown that (11) becomes

$$2\pi w_{bL}=\int_0^\infty \dot{D}e^{-pt}\int_r^\infty \frac{ne^{-pn}}{\sqrt{(n^2-r^2)}}\frac{1}{r}\frac{dr}{dN}\,dndt \tag{12}$$

$$r=\sqrt{[(\bar{x}-X)^2+(\bar{y}-Y)^2]},$$

$$\frac{dr}{dN}=\frac{1}{r}\frac{dX}{dS}[\bar{y}-Y+Y'(\bar{x}-X)] \tag{13}$$

where dr/dN is the normal derivative of the distance r along the dislocation edge path. The inverse Laplace transform follows by inspection as

$$2\pi w_b=\int_0^\infty \frac{\dot{D}H(\tau-r)}{\sqrt{(\tau^2-r^2)}}\frac{\tau}{r}\frac{dr}{dN}dt,\quad \tau=s-t \tag{14}$$

By recognizing a first integral w.r.t. s, equation (14) can be rewritten as

$$w_b=\dot{W},\quad 2\pi W=\int_0^\infty \dot{D}H(\tau-r)\sqrt{(\tau^2-r^2)}\frac{1}{r}\frac{dr}{dN}dt \tag{15}$$

so that, from (4)

$$\tau_{yb}=\mu\dot{G},\quad G=W_{,y} \tag{16}$$

In light of (1), W can be viewed as a function of (ϕ,Ω) and it can be shown that along $y=0$

$$G(x,s)=-\frac{1}{x}\frac{\partial W}{\partial\phi}(\phi,\Omega) \tag{17}$$

The relationships (13) and (15)–(17) prove convenient in the next section.

Diffracted Stress Ahead of Crack

The problem (7) was also considered by Brock [8]. By following schemes by Kostrov [11] and Achenbach [12], the stress τ_{yc} for $y=0, x>0, s>d$ was found to be

$$\tau_{yc}(\xi,\eta)=\frac{1}{\pi\sqrt{(\eta-\xi)}}\int_{L(\xi)}^{\xi}\tau_{yb}(\xi,u)\frac{\sqrt{(\xi-u)}}{\eta-u}du \tag{18}$$

$$L(\xi)=\frac{d}{\sqrt{2}}\left(\frac{d+\sqrt{2}\xi\cos\psi}{\sqrt{2}\xi+d\cos\psi}\right),\quad \sqrt{2}\xi=s-x,\quad \sqrt{2}\eta=s+x \tag{19}$$

where $\sqrt{2}\xi>d$, $\eta>\xi$. Here (ξ,η) are characteristic coordinates, u is an integration variable representing η-dependence, and $\eta=L(\xi)$ defines in the $\xi\eta$-plane the shear wave front radiating from the equilibrium dislocation edge position. In view of (16), (17), (19), and the fact that G vanishes along the wave front, equation (18) can be rewritten as

$$\frac{1}{\mu}\tau_{yc}(\xi,\eta)=\frac{1}{\pi\sqrt{(\eta-\xi)}}\frac{\partial}{\partial s}\int_{L(\xi)}^{\xi}G\left[\frac{1}{\sqrt{2}}(u-\xi),\frac{1}{\sqrt{2}}(u+\xi)\right]\frac{\sqrt{(\xi-u)}}{\eta-u}\,du\quad (x>0,s\geq d) \tag{20}$$

Dynamic Stress Intensity Factor

By introducing (1), (13), (15), and (17) with $y=0$ and the variable change $\sqrt{2}z=\xi-u$ while noting that the integration order in the zt-plane can be interchanged, equation (20) can be rewritten as

$$\frac{2\pi^2}{\mu}\tau_{yc}(x,s)=\frac{-1}{\sqrt{x}}\frac{\partial}{\partial s}\int_0^{t^*}\dot{D}\frac{dX}{dS}\sqrt{2}\frac{\partial}{\partial\phi}\sqrt{(\tau+U)}\int_0^Z\frac{\sqrt{(Z-z)}}{(x+z)\sqrt{z}}\frac{1}{r^2}(C-BY')dzdt \tag{21}$$

$$B=d\cos\Omega+z\sin\phi-X,\quad C=d\sin\Omega+z\cos\phi-Y \tag{22}$$

$$Z=\frac{1}{2}\frac{\tau^2-R^2}{\tau+U},\quad R=\sqrt{(U^2+V^2)}=\sqrt{[d^2+X^2+Y^2-2d(X\cos\Omega+Y\sin\Omega)]} \tag{23}$$

$$U=d\cos\psi-X\cos\phi-Y\sin\phi,\quad V=d\sin\psi-X\sin\phi+Y\cos\phi \tag{24}$$

where $t^*=s-R(t^*)$. The restrictions on $(D,\dot{D},Y)$ imply that $t^*=0$ for $s=d$ and $dt^*/ds\geq 0$, $0\leq t^*\leq s$ for $s\geq d$. Figure 2 illustrates that $(x,y)=(U,V)$ and R are, respectively, the instantaneous dislocation edge position and instantaneous distance between the crack and dislocation edges. Thus, $R(0)=d$.

The z-integrand behaves as $0(z^{-2})$ for $|z|\to\infty$, has branch points at $(0,Z)$, simple poles at $-U\pm i|V|$ $(r^2=0)$, and a first-order singularity on the branch cut at $-x(x>0)$. These observations allow use of the Cauchy residue theorem to perform the z-integration. The ϕ and s-differentiations can then readily be carried out and it can be shown that for $x\to 0$, $s\geq d$

$$\frac{1}{\mu}\tau_{yc}(x,s)\sim\frac{K_c(t^*)}{2\sqrt{(xd)}} \tag{25}$$

$$\pi K_c(t^*)=\frac{-\dot{D}}{1-\dot{D}\cos(\omega-\theta)}\sqrt{\left(\frac{d}{R}\right)}\frac{dX}{dS}\sin(\omega-\theta)\sin\frac{\theta}{2}-\frac{1}{2d}\int_0^{t^*}\dot{D}\frac{dX}{dS}\sqrt{\left(\frac{d}{R}\right)^3}I(t)dt\quad (s\geq d) \tag{26}$$

$$I(t)=\cos\left(\phi-\frac{3\theta}{2}\right)+Y'\sin\left(\phi-\frac{3\theta}{2}\right) \tag{27}$$

$$\omega=\phi-\alpha,\quad \tan\theta=\frac{V}{U},\quad \tan\alpha=Y'\ (|\theta|\leq\pi,|\alpha|\leq\pi/2) \tag{28}$$

Figure 2 shows that (R,θ) are the plane polar coordinates of the instantaneous dislocation edge position w.r.t. the crack edge, α is its instantaneous slope w.r.t. the initial dislocation plane, and $-\omega$ is the instantaneous slope w.r.t. the crack plane. Thus, $\theta(0)=\psi$ and $\omega(0)=\phi$. Again it is understood that $Y=Y(X)$, $X=X(D)$, while $(D,\dot{D})$ are functions of t. Upon introduction of the trajectory length integration variable

$$\int_0^{X[D(t)]}\sqrt{[1+(Y')^2]}du \tag{29}$$

in view of (2), (10b), and the restrictions on Y it can be shown that

$$\frac{1}{2d}\dot{D}\frac{dX}{dS}\sqrt{\left(\frac{d}{R}\right)^3}I(t)=\frac{d}{dN}\left[\sqrt{\left(\frac{d}{R}\right)}\sin\frac{\theta}{2}\right]$$

$$=\frac{d}{dS}\left[\sqrt{\left(\frac{d}{R}\right)}\cos\frac{\theta}{2}\right] \tag{30}$$

Then, equation (26) assumes the form

$$\pi K_c(t^*)=\cos\frac{\psi}{2}-\sqrt{\left(\frac{d}{R}\right)}\cos\frac{\theta}{2}$$

$$-\frac{\dot{D}}{1-\dot{D}\cos(\omega-\theta)}\sqrt{\left(\frac{d}{R}\right)}\sin(\omega-\theta)\sin\frac{\theta}{2}\quad(s\geq d) \tag{31}$$

An alternative form can be obtained by noting that

$$\sin(\omega-\theta)=-\frac{dR}{dN},\quad \cos(\omega-\theta)=-\frac{dR}{dS} \tag{32}$$

The form of K_c is independent of (29) so that, as indicated earlier, the single-valuedness restriction on the trajectory function Y can be dropped and the slope angle α can take on values $|\alpha|\leq\pi$. Equation (31) appropriately reduces to the results in [8] for rectilinear motion ($\alpha\equiv 0$).

In view of (5), the dynamic stress intensity factor K for the problem is obtained by superposing K_c on the equilibrium intensity factor K_0. It is readily shown [4] that πK_0 is the negative of the first term in (31) so that

$$\pi K(t^*)=-\sqrt{\frac{d}{R}}\frac{\cos\frac{\theta}{2}+\dot{D}\cos\left(\omega-\frac{\theta}{2}\right)}{1-\dot{D}\cos(\omega-\theta)} \tag{33}$$

Equation (33) is convenient for computational purposes. In the following analysis, however, alternative forms prove to be useful.

General Observations on K

Equation (33) shows that the dynamic stress intensity factor depends explicitly on the instantaneous dislocation position (R,θ), orientation (ω), and speed $(\dot{D})$. In Fig. 2 the angle β between the radial (R) and tangential (S) directions is defined as

$$\beta=\pi+(\omega-\theta)\text{sgn}(\theta)\quad(0\leq\beta\leq\pi) \tag{34}$$

It should be noted that β, unlike the angles $(\theta,\ \psi,\ \phi,\ \alpha)$, is measured w.r.t. instantaneous directions and thus, for convenience, has no positive or negative sense in the xy-plane. In view of (31) and (34), equation (33) becomes

$$\pi K(t^*)=-\sqrt{\frac{d}{R}}\frac{\cos\frac{\theta}{2}+\dot{D}\cos\left(\beta+\left|\frac{\theta}{2}\right|\right)}{1+\dot{R}} \tag{35}$$

where $\dot{D}\sin\beta$ and $\dot{R}=\dot{D}\cos\beta$ are, respectively, the dislocation velocity components in the directions perpendicular and parallel to the R-direction. Equation (35) can itself be rewritten as

$$\pi K(t^*)=\sqrt{\frac{d}{R}}\left(-\cos\frac{\theta}{2}+\frac{\dot{D}\sin\beta}{1+\dot{R}}\sin\left|\frac{\theta}{2}\right|\right) \tag{36}$$

which shows that the intensity factor has two competing (of opposite sign) components. The first component depends on the dislocation position, while explicit orientation and speed dependence is coupled with positional dependence in the second component. Both components vary inversely with the distance between the dislocation and crack edge. However, while the first component varies directly with the angle between the distance line and the crack surface, variation of the second component is inverse. Thus, these components vanish, respectively, on the crack surface and directly ahead of the crack edge. The second component also vanishes when the dislocation moves directly toward or away from the crack edge $(\beta=0,\pi)$. These observations imply that the intensity factor is finite except perhaps when the dislocation is at the crack edge $(R=0)$ and may vanish for various combinations of dislocation position, orientation, and speed.

Figure 1 shows that the dislocation at some $t_a>0$ will radiate a shear wave that travels the distance $R(t_a)$ to subsequently reach the crack edge at $s_a=t_a+R(t_a)$. Similarly, the dislocation at some $t_b>t_a$ will radiate a shear wave that reaches the crack edge at $s_b=t_b+R(t_b)$. If $t_b=t_a+\epsilon$, $0<\epsilon<<d$, then from (23)

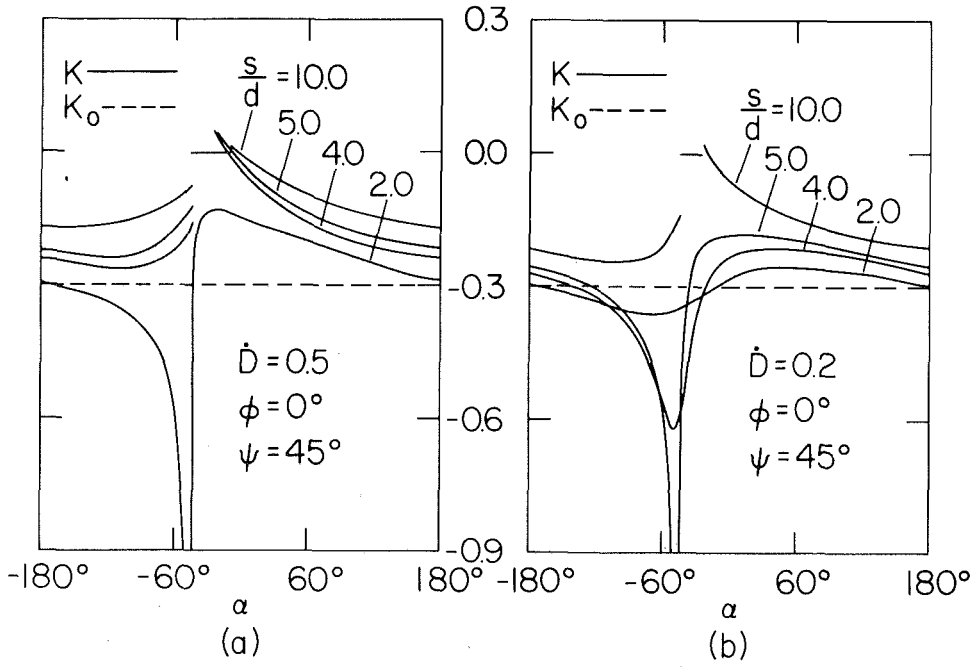

Fig. 3 (a) K versus α, $\dot{D}=0.5$; and (b) K versus α, $\dot{D}=0.2$

$$s_b - s_a = t_b - t_a + R(t_b) - R(t_a) \sim [1 + \dot{R}(t_a)]\epsilon,$$

$$\dot{R} = \frac{\dot{D}}{R}\frac{dX}{dS}[X - d\cos\Omega + Y'(Y - d\sin\Omega)] \tag{37}$$

The condition $\dot{D} < 1$ and (10*b*) guarantee that $|\dot{R}| < 1$, and the left-hand side of (37) is therefore positive. Thus, the order in which signals giving rise to K leave the dislocation is preserved, on their arrival at the crack edge.

With this in mind, we now consider dislocation motion discontinuities: Suppose that the dislocation speed undergoes a sudden change at $t = t_0$. Since $dt^*/ds \geq 0$, $0 < t^* < s$, we have $t^* = t_0$ at some subsequent instant $s_0 = t_0 + R(t_0)$. Since $\dot{D}$ is finite and the path is continuous, the first intensity factor component will be continuous at s_0. However, the second will instantaneously change unless $\beta = \pi/2$ and $\theta = 0$ at t_0, i.e., the dislocation was crossing directly ahead of the crack edge at right angles to the crack plane.

A related phenomenon occurs when the dislocation arrests or starts moving at t_0. The intensity factor will suffer a discontinuity as s_0 unless at t_0 $\beta = \pi/2$ and $\theta = 0$ or $\dot{D}$ vanishes continuously. If arrest occurs, only the first component remains and gives K the constant value

$$\pi K = -\sqrt{\frac{d}{R(t_0)}}\cos\frac{\theta_{(t0)}}{2} \quad (s > s_0) \tag{38}$$

Thus, once the dislocation arrest signal reaches the crack edge, the intensity factor assumes a new equilibrium value. Since $\theta(t_0) = \pm\pi$, the intensity factor vanishes for $s > s_0$ when arrest is at any crack surface point except the edge. More generally, comparison of (36) and (38) shows that the first intensity factor component is essentially a static contribution. The second is a correction for dislocation motion not directly toward or away from the crack edge.

Dislocation motion discontinuities can also occur due to the path itself, which is required to be continuous but only piecewise smooth. If at some $t = t_0$ the dislocation reaches a corner, equations (33) and (35) show that unless $\dot{D}$ vanishes continuously there, an intensity factor discontinuity will subsequently be manifested at s_0 through the parameters (α, β, ω).

In summary, then, discontinuities in dislocation speed and path slope cause discontinuities in the dynamic stress intensity factor. However, appropriate behavior by either quantity can also remove the discontinuity effect due to the other.

Dynamic Overshoot

Because two components compete during dislocation motion, the signal received at the crack edge from a given dislocation position triggers in the dynamic analysis an intensity factor that will either have a smaller magnitude than the static value or be of opposite sign. Only when

$$\frac{\dot{D}\sin\beta}{1 + \dot{R}} > 2\cot\left|\frac{\theta}{2}\right|, \tag{39}$$

will the latter instance produce a larger magnitude. Thus, unless (39) is satisfied, dynamic overshoot in the sense that the dynamic stress intensity factor at some instant exceeds its initial equilibrium value occurs due to the change in dislocation position, e.g., the dislocation moves closer to the crack edge.

Numerical Illustrations

To illustrate the effect of the implicit orientation parameter α, we consider the dislocation motion defined by $(\dot{D}, \alpha)$ constant. The parameter K is plotted in Fig. 3(*a*) versus α for $\psi = 45$ deg, $\phi = 0$ deg, $\dot{D} = 0.5$, and various values of $s/d > 1.0$. The discontinuities for $\alpha = -45$ deg indicate dislocation arrest at the crack edge, which occurs when $s/d = 2.0$. The other discontinuities and the constant behavior show the aforementioned effects of dislocation arrest at other crack surface locations. In general, the K-variation with α decreases as s/d becomes large. As implied earlier K temporarily vanishes at several values of α. Figure 3(*b*) presents a K-plot for the same situation, except that now $\dot{D} = 0.2$ and crack edge arrest occurs for $\alpha = -45$ deg when $s/d = 5.0$. The observations made for Fig. 3(*a*) are apparently again valid. The decrease in K-variation with α, however, seems to occur more slowly.

In view of the behavior near and away from the value $\alpha = -45$ deg, Fig. 3 shows the inverse variation of the dynamic stress intensity factor magnitude with the distance between the dislocaton and crack edge. This behavior is more clearly illustrated in Fig. 4(*a*), where K is plotted versus $s/d \geq 1.0$ for

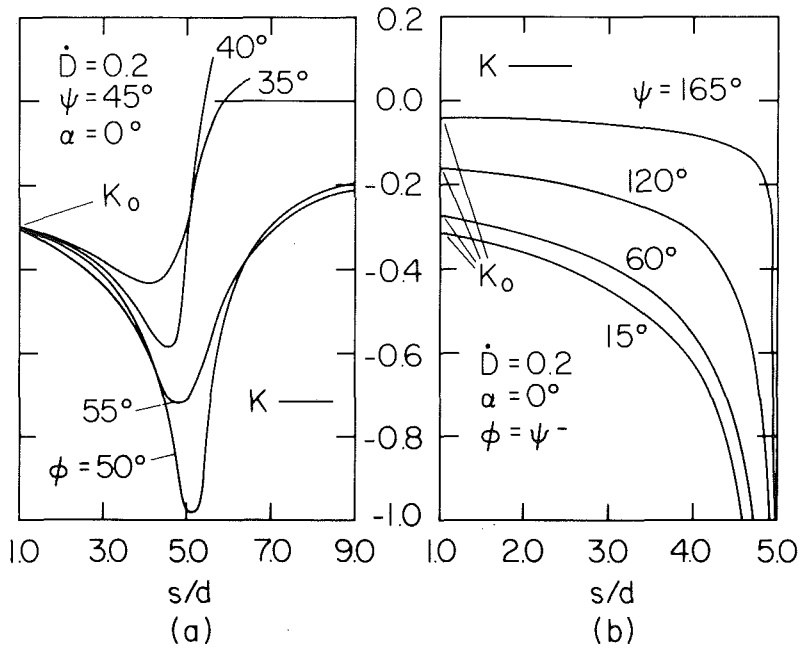

Fig. 4 (*a*) K versus s/d, $\psi = 45$ deg; and (*b*) K versus s/d, $\phi = \psi -$

$\dot{D}=0.2$, $\alpha=0$ deg, $\psi=45$ deg and $\phi=(35, 40, 50, 55$ deg). The intensity factor magnitude is seen to grow continuously until the dislocation nears its point of minimum distance to the crack edge. When the dislocation passes in front of the crack edge ($\phi=50, 55$ deg), the magnitude decreases asymptotically to zero. For the crack surface arrest cases ($\phi=35, 40$ deg) the intensity factor changes sign and then instantaneously vanishes when the arrest signals reach the crack edge.

As a third illustration, K is plotted in Fig. 4(*b*) versus $s/d \geq 1.0$ for $\dot{D}=0.2$, $\alpha=0$ deg and various values of ψ that define rectilinear paths which intersect the crack surface at the crack edge ($\phi=\psi^-$). Because $\beta \sim \pi$, the intensity factor motion component is negligible, and Fig. 4(*b*) shows the aforementioned characteristic that the static component varies inversely with the angle to the crack surface.

Application to Dynamic Fracture

Dynamic brittle fracture initiates at an existing crack under rapid loading conditions, such as stress wave diffraction at the crack edge [12]. If there are no other external stress fields, the crack in an ideal, homogeneous, isotropic solid is often treated as completely at rest prior to the stress wave arrival. In a real material, however, if a screw dislocation of strength h is located in equilibrium as in Fig. 1(*a*), and intensity factor k_0, where [4]

$$k_0 = -\frac{hK_0}{\sqrt{d}} = -\frac{h}{\pi\sqrt{d}}\cos\frac{\psi}{2} \tag{40}$$

will exist. An antiplane shear wave that subsequently ($s'=0$) diffracts at the crack edge will generate an additional intensity factor k_d. For the plane step-stress wave of magnitude σ in Fig. 5, it can be shown [13] that

$$g = \frac{k_d}{k_0} = \frac{\sigma}{\mu}\frac{d}{h}\frac{4\sqrt{(1-\sin\Phi)}}{\cos\frac{\psi}{2}}\sqrt{\frac{s'}{d}} \quad (s' \geq 0) \tag{41}$$

The dislocation strength is on the order of the atomic spacing in the cracked material. If it is argued that linear elasticity breaks down very near the dislocation or that the large dislocation force does not allow equilibrium dislocations to exist very near the crack edge [4], then $|d/h| >> 1$. On the other hand, we require that $|\sigma/\mu| << 1$ in the elastic range; e.g., $|\sigma/\mu| \sim 0.0075$ for a hot-rolled low carbon steel at yield. The ratio of trigonometric terms can take on any value between 0 and ∞. Equation (41) shows, therefore, that the dislocation stress field can concievably govern ($|g| < 1$) the crack edge for a finite period. If $\sigma/h > 0$, then diffraction merely intensifies the existing (dislocation) stress field. If $\sigma/h < 0$, however, diffraction initially relaxes the crack edge stress field and subsequently reverses its sign. That is, the dislocation temporarily shields the crack edge from the wave diffraction effects, and so postpones the onset of a stress level critical for fracture. A discussion of this shielding concept has been presented for static situations in [4, 5].

If the wave diffraction process also triggers dislocation motion, the results of previous sections would modify (41) to give

$$g = \frac{\sigma}{\mu}\frac{d}{h}\frac{4(1+\dot{R})\sqrt{(1-\sin\Phi)}}{\cos\frac{\theta}{2}+\dot{D}\cos\left(\beta+\left|\frac{\theta}{2}\right|\right)}\sqrt{\frac{R}{d}}\sqrt{\frac{s'}{d}} \quad (s'>0) \tag{42}$$

$$s' + s_c = t^* + R(t^*) \geq d \tag{43}$$

Here $|s_c|$ is the interval between the arrival of the plane wave at the crack edge and dislocation motion initiation. The force on an equilibrium dislocation such as in Fig. 1(*a*) varies inversely with d and always points to the crack edge [4]. Therefore, if we ignore effects such as grain distortion or the plane wave itself and assume that the dislocation moves directly to the crack edge, previous analysis shows that the governance ratio g reduces to

$$g = \frac{\sigma}{\mu}\frac{d}{h}\frac{4\sqrt{(1-\sin\Phi)}}{\cos\frac{\psi}{2}}\sqrt{\frac{R}{d}}\sqrt{\frac{s'}{d}} \quad (s'>0) \tag{44}$$

The g-behavior versus s'/d for both stationary and moving dislocations is shown in Fig. 5 for various combinations of

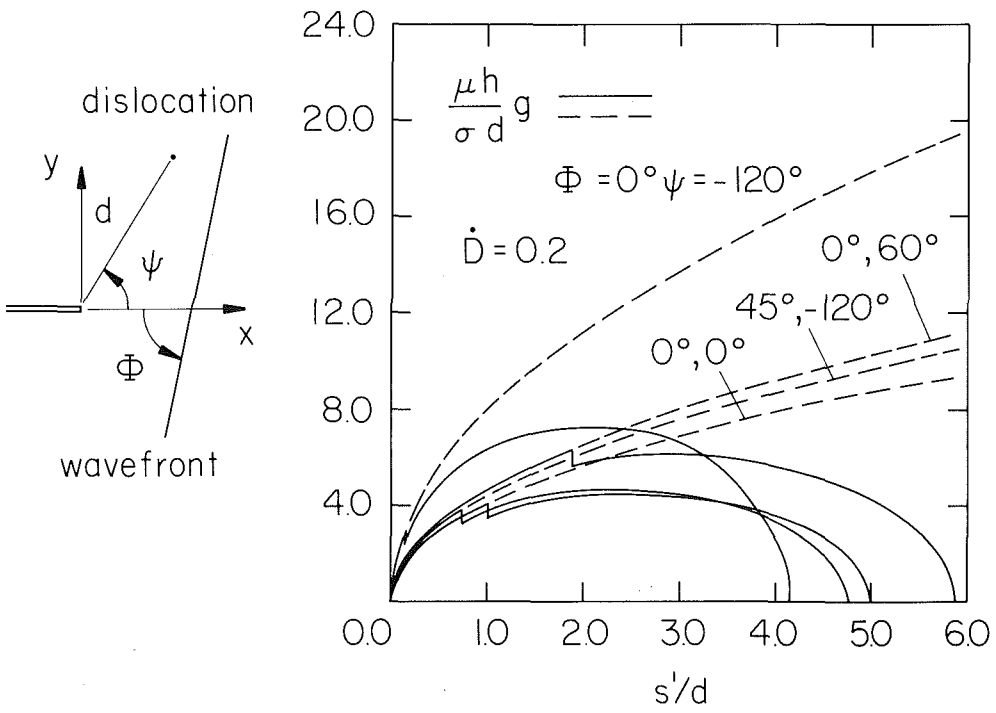

Fig. 5 *g* versus *s'/d*

(Φ,ψ). It is assumed that dislocation motion initiates on arrival of the wave pattern and proceeds at a constant speed $\dot{D}=0.2$. The discontinuities in Fig. 5 indicate the motion signal arrivals and the broken lines, the g-curves if no motion had occurred. The dislocation lies in the crack shadow when $\psi-\Phi>\pi/2$. Then, the diffracted cylindrical wave (see Figs. 1(b) and (c)) reaches the dislocation before the plane wave. If it is assumed that this wavefront has the same triggering effect, then $s_c=-d$ and $g=0$ for $s'/d<1.0$. The $(\Phi,\psi)-$ values chosen in Fig. 5 do not fall into this category.

Figure 5 shows that the stationary dislocation initially governs ($|g|<1$) the crack edge stress field. After a finite time that varies directly with $|\sigma d/\mu h|$ the wave diffraction governs ($|g|>1$) indefinitely, and to an ever-increasing degree. When dislocation motion occurs, however, the initial dislocation governance period may be increased while the wave diffraction governance interval is now finite, and may vanish entirely if $|\sigma d/\mu h|$ is large enough. Moreover, the degree of wave diffraction governance is lower than for the stationary dislocation at the same instant. In Fig. 5, the time intervals are on the order of the shear wave travel time d between the equilibrium dislocation and crack edge.

Figure 5 thus confirms the stationary dislocation observations. Because the dislocation-induced intensity factor itself increases with s' (inversely with R), Fig. 5 shows that these observations must be modified for the moving dislocation: For $\sigma/h>0$, the stress intensification process is accelerated, while for $\sigma/h<0$, the relaxation process might not occur ($|g|<1$) or will be briefer. Thus, a stress level critical for fracture will always be achieved sooner if the dislocation moves to the crack edge.

Since the time intervals arising here are on the order of shear wave travel times between the crack and equilibrium dislocation, the delay/acceleration effects for a single dislocation might not be readily detectable experimentally. However, a dislocation array might by superposition give measurable time intervals. On the other hand, the number of dislocations per grain has been estimated to be on the order of 10^{10}, which implies an unreasonably large k_0 total. However, this implication would follow from the assumption that h for each dislocation in the array is of the same sign. Finally, it should be noted that the results obtained here are for a dislocation existing initially in equilibrium. Wave excitation of the dislocation source itself involves the solution to the problem of the instantaneously appearing dislocation. This is related but not identical to the problem defined by (3) and (4).

Brief Summary

This paper first studied the dynamic stress intensity factor generated for a stationary crack by the motion of a screw dislocation of unit strength from an equilibrium position. The intensity factor was found to have two components of opposite sign. The first component depended on the instantaneous dislocation position. The second component also depended on the instantaneous dislocation speed and orientation, but vanished for the important case of a dislocation moving directly toward the crack edge. Discontinuities in the dislocation speed or a nonsmooth path were found to cause discontinuities in the intensity factor. However, appropriate behavior by either could remove the discontinuity effect due to the other. It was also found that dislocation arrest caused the intensity factor to instantaneously attain a new equilibrium value which, on the crack surface, vanishes.

More generally, the study showed that screw dislocation motion from rest near an otherwise undisturbed crack edge does not necessarily intensify or relax the stress field there. Stress field response depends on the dislocation path and speed, and how they affect the dislocation position in particular, the distance between the crack edge, and dislocation.

The study results were then used to consider a screw dislocation near a crack edge at which plane step-stress antiplane shear wave diffraction occurs. In terms of the combined intensity factor, it was found that, depending on the relation between the wave stress and the slip direction, a stationary screw dislocation can either accelerate or delay the onset of the stress level critical for crack edge fracture. If the wave pattern, however, also triggers dislocation motion into the crack edge, the delaying effect is diminished and the acceleration process accentuated. For a single dislocation, the time intervals involved are apparently on the order of the shear wave travel time between the equilibrium dislocation and the crack edge. The dimensionless quantity $\sigma d/\mu h$, the dislocation path angle ψ, and wavefront angle Φ are key parameters in determining these time intervals.

The results of this paper will form the basis for further studies of dynamic fracture in the presence of dislocations. In particular, future work will utilize more fully the path effect results obtained here; attempts to model the effects of crack edge and multiple dislocation interaction on the dislocation path in view of the dislocation force concept will be made. It is hoped, however, that the present results themselves will allow insight into this area.

References

1 Bilby, B. A., and Eshelby, J. D., "Dislocations and the Theory of Fracture," in: *Fracture*, Vol. 1, Liebowitz, H., ed. Academic Press, New York, 1968, Chapter 2.

2 Rice, J. R., and Thomson, R., "Ductile Versus Brittle Behaviour of Crystals," *Philosophical Magazine*, Vol. 29, 1974, pp. 73–97.

3 Tirosh, J., and McClintock, F. A., "Finding Elastoplastic Stress and Strain in Cracked Bars Under Torsion by Assembling Screw Dislocations," *Engineering Fracture Mechanics*, Vol. 11, 1979, pp. 563–572.

4 Majumdar, B. S., and Burns, S. J., "An Elastic Theory of Dislocation Arrays and Inclusions Near a Sharp Crack," Technical Report #2422-26, Department of Mechanical and Aerospace Sciences, University of Rochester, Rochester, N.Y., 1980.

5 Thomson, R. M., and Sinclair, J. E., "Mechanics of Cracks Screened by Dislocations," *Acta Metallurgica*, Vol. 30, 1982, pp. 1325–1334.

6 Johnston, W. G., and Gilman, J. J., "Dislocation Velocities, Dislocation Densities, and Plastic Flow in Lithium Fluoride Crystals," *Journal of Applied Physics*, Vol. 30, 1959, pp. 129–144.

7 Burridge, R., and Knopoff, L., "Body Force Equivalents for Seismic Dislocations," *Bulletin of the Seismological Society of America*, Vol. 54, 1964, pp. 1875–1888.

8 Brock, L. M., "The Dynamic Stress Intensity Factor for a Crack Due to Arbitrary Rectilinear Screw Dislocation Motion," *Journal of Elasticity*, to appear.

9 Sneddon, I. N., *The Use of Integral Transforms*, McGraw-Hill, New York, 1972.

10 deHoop, A. T., "A Modification of Cagniard's Method for Solving Seismic Pulse Problems," *Applied Scientific Research*, Vol. B8, 1960, pp. 349–356.

11 Kostrov, B. V., "Unsteady Propagation of Longitudinal Shear Cracks," *Prikladnaya Matem i Mekhanika*, Vol. 30, 1966, pp. 1241–1248 (English translation).

12 Achenbach, J. D., *Wave Propagation in Elastic Solids*, North-Holland, Amsterdam, 1973, Chapter 9.

13 Brock, L. M., "Effects of Secondary Diffractions on the Stress Intensity Factors Generated for a Finite Crack by a Shear Wave," *International Journal of Engineering Science*, Vol. 13, 1975, pp. 851–859.